optica

Super-resolution quantum imaging at the Heisenberg limit: supplementary material

MANUEL UNTERNÄHRER[1,*], BÄNZ BESSIRE[1], LEONARDO GASPARINI[2], MATTEO PERENZONI[2], AND ANDRÉ STEFANOV[1]

[1] Institute of Applied Physics, University of Bern, 3012 Bern, Switzerland
[2] Fondazione Bruno Kessler FBK, 38122 Trento, Italy
[*] Corresponding author: umanuel@gmail.com

Published 20 September 2018

This document provides supplementary information to "Super-resolution quantum imaging at the Heisenberg limit," https://doi.org/10.1364/OPTICA.5.001150. The main theoretical results of OCM imaging are here formally derived. In addition, an incoherent imaging version with equal resolution improvement is proposed. The physical model of the experimental OCM quantum state generation based on SPDC is worked out. An analysis of the resolution scaling of classically correlated photons is shown to be at the standard quantum limit and provides for this case a classical limit of the point-spread-function. Additional measurements of the generated quantum state further verify the theoretical model and demonstrate the capability of the newly developed detector array.

1. DERIVATION OF THE OCM IMAGING EQUATION

This section provides a step-by-step derivation of Eq. (3) and Eq. (4) of the article. Starting from the N-th order correlation function in the image plane

$$G^{(N)}(\boldsymbol{\rho}_1,...,\boldsymbol{\rho}_N) = \left| \int d^2\boldsymbol{\rho}'_1 \dots d^2\boldsymbol{\rho}'_N \, A\left(\frac{\boldsymbol{\rho}'_1 + \dots + \boldsymbol{\rho}'_N}{N}\right) h\left(\frac{\boldsymbol{\rho}_1}{m} - \boldsymbol{\rho}'_1\right) \dots h\left(\frac{\boldsymbol{\rho}_N}{m} - \boldsymbol{\rho}'_N\right) \right|^2,$$

where the simplification of setting the magnification to $m = 1$ does not limit the generality of the following result. A coordinate change to the centroid and deviation variables

$$\boldsymbol{X} = \frac{1}{N}\sum_{k=1}^{N} \boldsymbol{\rho}_k, \quad \boldsymbol{\xi}_k = \boldsymbol{\rho}_k - \boldsymbol{X}, \; k \in \{1,\dots,N\}$$

yields for the integral in the modulus

$$N^2 \int d^2\boldsymbol{X}' d^2\boldsymbol{\xi}'_1 \dots d^2\boldsymbol{\xi}'_{N-1} \, A(\boldsymbol{X}') \, h\left(\boldsymbol{X} + \boldsymbol{\xi}_1 - (\boldsymbol{X}' + \boldsymbol{\xi}'_1)\right) \dots h\left(\boldsymbol{X} + \boldsymbol{\xi}_N - (\boldsymbol{X}' + \boldsymbol{\xi}'_N)\right).$$

The Jacobian determinant of this coordinate transformation can be readily shown to be $|\det J| = |\det J_x| \cdot |\det J_y| = N^2$ and is present as a prefactor. By a change of variables to $\boldsymbol{\xi}''_k = \boldsymbol{\xi}_k - \boldsymbol{\xi}'_k$, we get

$$\int d^2\boldsymbol{X}' A(\boldsymbol{X}') \left(N^2 \int d^2\boldsymbol{\xi}''_1 \dots d^2\boldsymbol{\xi}''_{N-1} \, h\left(\boldsymbol{\xi}''_1 + \boldsymbol{X} - \boldsymbol{X}'\right) \dots h\left(\boldsymbol{\xi}''_N + \boldsymbol{X} - \boldsymbol{X}'\right) \right).$$

The term in parentheses is a function $H(\boldsymbol{X} - \boldsymbol{X}')$ and serves as an effective OCM PSF. Therefore

$$H(\boldsymbol{X}) = N^2 \int d^2\boldsymbol{\xi}_1 h(\boldsymbol{\xi}_1 + \boldsymbol{X}) \dots \int d^2\boldsymbol{\xi}_{N-1} h(\boldsymbol{\xi}_{N-1} + \boldsymbol{X}) \, h\left(\boldsymbol{\xi}_N + \boldsymbol{X}\right).$$

Due to $\sum_k \boldsymbol{\xi}_k = 0$ we can infer $\boldsymbol{\xi}_N = -\sum_{k=1}^{N-1} \boldsymbol{\xi}_k$. By defining the notation $h^{*k} \doteq (h * \ldots * h)$ for the k-times repeated self-convolution of a function $h = h^{*1}$, we can deduce

$$\begin{aligned} H(\boldsymbol{X}) &= N^2 \int d^2\boldsymbol{\xi}_1\, h(\boldsymbol{\xi}_1 + \boldsymbol{X}) \ldots \int d^2\boldsymbol{\xi}_{N-1}\, h(\boldsymbol{\xi}_{N-1} + \boldsymbol{X})\, h\left(\boldsymbol{X} - \sum_{k=1}^{N-1} \boldsymbol{\xi}_k\right) \\ &= N^2 \int d^2\boldsymbol{\xi}_1\, h(\boldsymbol{\xi}_1 + \boldsymbol{X}) \ldots \underbrace{\int d^2\boldsymbol{\xi}'_{N-1}\, h(\boldsymbol{\xi}'_{N-1})\, h\left(2\boldsymbol{X} - \sum_{k=1}^{N-2} \boldsymbol{\xi}_k - \boldsymbol{\xi}'_{N-1}\right)}_{h^{*2}\left(2\boldsymbol{X} - \sum_{k=1}^{N-2} \boldsymbol{\xi}_k\right)} \\ &= N^2 \int d^2\boldsymbol{\xi}_1\, h(\boldsymbol{\xi}_1 + \boldsymbol{X}) \ldots \int d^2\boldsymbol{\xi}_{N-2}\, h(\boldsymbol{\xi}_{N-2} + \boldsymbol{X})\, h^{*2}\left(2\boldsymbol{X} - \sum_{k=1}^{N-2} \boldsymbol{\xi}_k\right) \\ &= \ldots = N^2 \int d^2\boldsymbol{\xi}_1\, h(\boldsymbol{\xi}_1 + \boldsymbol{X})\, h^{*(N-1)}\left((N-1)\boldsymbol{X} - \boldsymbol{\xi}_1\right) \\ &= N^2\, h^{*N}(N\boldsymbol{X}) \end{aligned} \tag{S1}$$

This is the result of Eq. (4) of the article. The OCM PSF can be written as N-times repeated self-convolution of the PSF $h(\boldsymbol{\rho})$ of the optical system. For a general magnification factor m, we have therefore derived

$$G^{(N)}(\boldsymbol{X}, \boldsymbol{\xi}_1, \ldots, \boldsymbol{\xi}_{N-1}) = \left| \int d^2\boldsymbol{X}'\; A\left(\boldsymbol{X}'\right) H\left(\frac{\boldsymbol{X}}{m} - \boldsymbol{X}'\right) \right|^2 = \left| (A * H)\left(\frac{\boldsymbol{X}}{m}\right) \right|^2 .$$

For the single lens PSF $h(\boldsymbol{\rho}) = \mathrm{jinc}(2\pi R|\boldsymbol{\rho}|/s_o\lambda)$, the result of $H(\boldsymbol{X}) = N^2\, h^{*N}(N\boldsymbol{X})$ in Eq. (5) of the article

$$H(\boldsymbol{X}) = C\,\mathrm{jinc}\left(\frac{2\pi RN}{s_o\lambda}|\boldsymbol{X}|\right)$$

can be understood in terms of a Fourier transform version of Eq. (S1). With the Fourier transform $\tilde{h}(\boldsymbol{q})$ of $h(\boldsymbol{\rho})$ in transverse wavevector coordinates $\boldsymbol{q}$, Eq. (S1) is equivalent to

$$H(\boldsymbol{X}) = \frac{N^2}{(2\pi)^2} \int d^2\boldsymbol{q}\;\; \left(\tilde{h}(\boldsymbol{q})\right)^N e^{iN\boldsymbol{q}\cdot\boldsymbol{X}}.$$

As $\tilde{h}(\boldsymbol{q})$ is given by the lens pupil function [1], any power of it is of unity transmission amplitude within its circular region. This results in a N-times narrower but otherwise equal PSF as for classical imaging. Note that for a Gaussian pupil function (apodization), the centroid PSF narrows only with $1/\sqrt{N}$, corresponding to the SQL.

2. INCOHERENT OCM IMAGING

The OCM state of Eq. (2) in the article with a sharp centroid position at location $\boldsymbol{X}_0$ can be gained by replacing $A(\boldsymbol{\rho}) \to A_{\boldsymbol{X}_0}(\boldsymbol{X}) = \delta^{(2)}(\boldsymbol{X} - \boldsymbol{X}_0)$. This state shall be denoted by

$$|\Psi_{\boldsymbol{X}_0}\rangle = \int d^2\boldsymbol{\rho}_1 \ldots d^2\boldsymbol{\rho}_N\; \delta^{(2)}\left(\frac{\boldsymbol{\rho}_1 + \ldots + \boldsymbol{\rho}_N}{N} - \boldsymbol{X}_0\right) |\boldsymbol{\rho}_1, \ldots, \boldsymbol{\rho}_N\rangle .$$

For an object aperture function $A(\boldsymbol{\rho})$, the mixed state given by the density operator

$$\rho = \int d^2\boldsymbol{X}\, |A(\boldsymbol{X})|^2\; |\Psi_{\boldsymbol{X}}\rangle\, \langle\Psi_{\boldsymbol{X}}|$$

contains an incoherent image. It is straightforward to show using the results of section 1 that with this mixed state as an input in plane Σ_o of setup in Fig. 1, the correlation function in Σ_i will read

$$G^{(N)}(\boldsymbol{X}, \boldsymbol{\xi}_1, \ldots, \boldsymbol{\xi}_{N-1}) = \int d^2\boldsymbol{X}' \left| A\left(\boldsymbol{X}'\right) H\left(\frac{\boldsymbol{X}}{m} - \boldsymbol{X}'\right) \right|^2 = \left(|A|^2 * |H|^2\right)\left(\frac{\boldsymbol{X}}{m}\right).$$

This is formally analogues to classical incoherent imaging. The image is formed point-by-point, no interferences can occur.

This imaging could be realised in our experimental implementation by focusing the pump beam in the object plane Σ'_o and randomly scanning over the aperture. This classical randomness would produce the mixed state described above. Tsang proposed in [2] such a scheme using a quantum "laser pointer" to build up an image incoherently at super-resolution. A disadvantage is that the single-shot property of the state generation would be lost in such an approach.

3. OCM STATE GENERATION USING SPDC

This section derives Eq. (7), the biphoton state at the output plane of the state preparation. Assuming narrow-band pumping and fixed detection wavelengths realized by spectral filtering, the generated biphoton state at the central plane of the NLC reads

$$|\Psi\rangle = \int d^2\boldsymbol{q}_s d^2\boldsymbol{q}_i \, \tilde{E}_p\left(\boldsymbol{q}_s + \boldsymbol{q}_i\right) \operatorname{sinc}\left(\frac{\Delta k\, L}{2}\right) |\boldsymbol{q}_s, \omega_s\rangle \, |\boldsymbol{q}_i, \omega_i\rangle \tag{S2}$$

in transverse wavevector coordinates $\boldsymbol{q}_s$ and $\boldsymbol{q}_i$ for the signal and idler photon at their corresponding angular frequencies ω_s and ω_i, and the pump field distribution $\tilde{E}_p(\boldsymbol{q})$ at angular frequency ω_p [3]. Energy conservation imposes $\omega_p = \omega_s + \omega_i$. The wavevector mismatch

$$\Delta k = \sqrt{\left(\frac{\omega_s}{c} n(\omega_s)\right)^2 - \boldsymbol{q}_s^2} + \sqrt{\left(\frac{\omega_i}{c} n(\omega_i)\right)^2 - \boldsymbol{q}_i^2} - \sqrt{\left(\frac{\omega_s + \omega_i}{c} n(\omega_s + \omega_i)\right)^2 - (\boldsymbol{q}_s + \boldsymbol{q}_i)^2} + \frac{2\pi}{G}$$

where c is the speed of light and the refractive index $n(\omega)$ of the crystal is given by its temperature dependant Sellmeier equations. The NLC poling period G is fixed at its fabrication and is chosen to achieve $\Delta k = 0$ at the used wavelengths and for collinear emission $\boldsymbol{q} = 0$.

Let the function $E_o(\boldsymbol{\rho})$ define the electric field distribution of the monochromatic pump of angular frequency ω_p in the object plane Σ_o' of Fig. 1. Propagating it trough the first lens of focal length f to the center of the crystal, the far-field plane relative to Σ_o', the field distribution is given by $E_p(\boldsymbol{\rho}) = \tilde{E}_o\left(\omega_p \boldsymbol{\rho}/cf\right)$ with the Fourier transform $\tilde{E}_o(\boldsymbol{q}) = \int d\boldsymbol{\rho}\, E_o(\boldsymbol{\rho})\, e^{-i\boldsymbol{q}\boldsymbol{\rho}}$ [1]. Therefore, this pump field incident on the NLC has a Fourier transform of

$$\tilde{E}_p(\boldsymbol{q}) = E_o\left(-\frac{cf}{\omega_p}\boldsymbol{q}\right) \tag{S3}$$

and can be inserted in Eq. (S2).

The SPDC state has to be propagated from the NLC through the lens of focal length f to the output plane Σ_o. The latter is the far-field plane relative to the NLC central plane. Plane waves of transversal wavevector $\boldsymbol{q}$ emitted by the NLC are focused to a location $\boldsymbol{\rho} = \frac{cf}{\omega}\boldsymbol{q}$ [1]. Formally, the state propagation can be performed by the transformation $|\boldsymbol{q}, \omega\rangle \to |\frac{cf}{\omega}\boldsymbol{q} = \boldsymbol{\rho}, \omega\rangle$. Using Eq. (S3) and Eq. (S2), we get

$$|\Psi\rangle = \int d^2\boldsymbol{\rho}_s d^2\boldsymbol{\rho}_i \, E_o\left(-\frac{\omega_s\boldsymbol{\rho}_s + \omega_i\boldsymbol{\rho}_i}{\omega_s + \omega_i}\right) \operatorname{sinc}\left(\frac{\Delta k\, L}{2}\right) |\boldsymbol{\rho}_s, \omega_s\rangle \, |\boldsymbol{\rho}_i, \omega_i\rangle \tag{S4}$$

where Δk is evaluated at $\boldsymbol{q}_k = (\omega_k/cf)\boldsymbol{\rho}_k$, $k \in \{s, i\}$. For frequency degenerated emission with $\omega_s = \omega_i = \frac{1}{2}\omega_p$, the biphoton state in the preparation output plane Σ_o reads

$$|\Psi\rangle = \int d^2\boldsymbol{\rho}_s d^2\boldsymbol{\rho}_i \, E_o\left(-\frac{\boldsymbol{\rho}_s + \boldsymbol{\rho}_i}{2}\right) \operatorname{sinc}\left(\frac{\Delta k\, L}{2}\right) |\boldsymbol{\rho}_s, \tfrac{1}{2}\omega_p\rangle \, |\boldsymbol{\rho}_i, \tfrac{1}{2}\omega_p\rangle \, .$$

Finally, uniformly illuminating an object aperture $A(\boldsymbol{\rho})$ in the plane Σ_o' yields $E_o(\boldsymbol{\rho}) = A(\boldsymbol{\rho})$.

Eq. (S4) shows the necessity to filter for frequency degenerate emission in order to properly reconstruct the image with the centroid. Broadband emission could be conceived if the detection provides spectral information.

4. STANDARD QUANTUM LIMIT OF CLASSICALLY CORRELATED PHOTONS

This section derives a centroid PSF for classically correlated photons with no entanglement and shows its behaviour at large photon number N. For simplicity, we set first $N = 2$. Assuming OCM-like correlations for a point object, in the object plane these are modelled by a classical, multi-variate probability density function

$$p_o(\boldsymbol{\rho}_1, \boldsymbol{\rho}_2) = \delta^{(2)}(\boldsymbol{\rho}_1 + \boldsymbol{\rho}_2).$$

Propagating the photons through the resolution limited imaging system, the process of blurring by the PSF can be described by adding a random variable $\boldsymbol{N}$ to their original positions in the object plane

$$\boldsymbol{\rho}_k \to \boldsymbol{\rho}_k + \boldsymbol{N}_k, \quad k \in \{1, 2\}.$$

As both photons are affected by the PSF independently, a separate random spread term is needed for each. Their probability density function is given by the PSF of the imaging system with $P_{N_k}(\boldsymbol{N}) = |h(\boldsymbol{N})|^2$. Using elementary statistics, we get for the probability density in the image plane

$$\begin{aligned} p_i(\boldsymbol{\rho}_1, \boldsymbol{\rho}_2) &= \int d^2\boldsymbol{\rho}_1' d^2\boldsymbol{\rho}_2' \, p_o(\boldsymbol{\rho}_1, \boldsymbol{\rho}_2) \, |h(\boldsymbol{\rho}_1 - \boldsymbol{\rho}_1')|^2 \, |h(\boldsymbol{\rho}_2 - \boldsymbol{\rho}_2')|^2 \\ &= \left(|h|^2 * |h|^2\right)(\boldsymbol{\rho}_1 + \boldsymbol{\rho}_2). \end{aligned}$$

This is formally equivalent to independent, incoherent imaging of the photons and therefore validates the statistical model assumed. Using $\boldsymbol{\rho}_- = \frac{1}{2}(\boldsymbol{\rho}_1 - \boldsymbol{\rho}_2)$, the centroid random variable $\boldsymbol{X}_i$ in the image plane has a probability density function

$$P_{\boldsymbol{X}_i}(\boldsymbol{X}) = \int d^2\boldsymbol{\rho}_- \, p_i(\boldsymbol{X} + \boldsymbol{\rho}_-, \boldsymbol{X} - \boldsymbol{\rho}_-) = \int d^2\boldsymbol{\rho}_- \, \left(|h|^2 * |h|^2\right)(2\boldsymbol{X}) \propto \left(|h|^2 * |h|^2\right)(2\boldsymbol{X}).$$

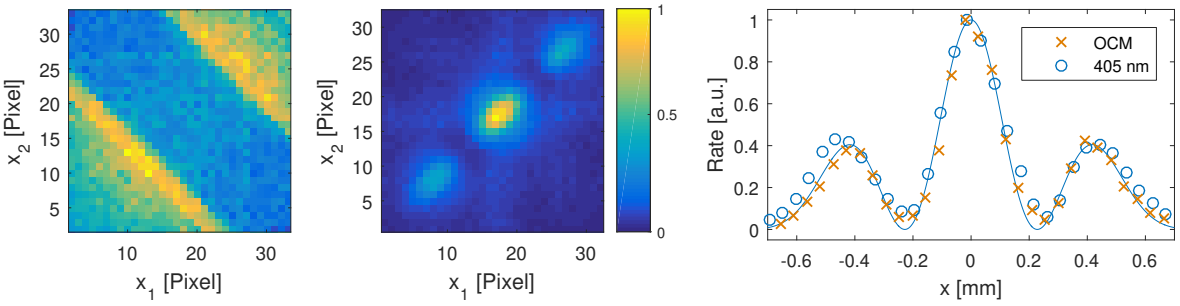

(a) Near-Field Correlations (b) Far-Field Correlations (c) Far-Field, OCM Diagonal vs. 405 nm

Fig. S1. The biphoton OCM state of a double-slit is analyzed in near- and far-field for position-correlations in x-direction orthogonal to the lines. The high NA near-field measurement in (a) shows the image features on the diagonals and thereby in the centroid position. In far-field (b), strong correlation is observed. (c) shows the diagonal of this OCM diffraction pattern (orange crosses) and the expected narrowing down to the width produced with coherent light at 405 nm (blue circles). The theoretical curve for the latter is shown.

Generalizing to a classically correlated N-photon state, on can use the fact that the centroid random variable in the image plane is

$$\boldsymbol{X}_i = \frac{1}{N}\left(\sum_{k=1}^{N} \boldsymbol{\rho}_k + \boldsymbol{N}_k\right).$$

With the OCM property $\sum_{k=1}^{N} \boldsymbol{\rho}_k = 0$ of a point object at the origin, we can conclude that the probability distribution of $\boldsymbol{X}_i$ is given by the sum of N independent noise sources and reads

$$P_{\boldsymbol{X}_i}(\boldsymbol{X}) = \left(|h|^2\right)^{*N}(N\boldsymbol{X}) \tag{S5}$$

using the self-convolution notation from Sec. 1. This is the PSF of classical OCM imaging and the optimum for any imaging using classically correlated photons.

Because the noise terms are independent, identically distributed random variables, we can apply the central limit theorem of probability theory. This says, that the probability density of Eq. (S5) converges in the limit of large N to a normal distribution

$$P_{\boldsymbol{X}_i}(\boldsymbol{X}) \xrightarrow{N\to\infty} \frac{1}{\sqrt{2\pi\sigma^2/N}}\, e^{-\frac{x^2}{2\sigma^2/N}}$$

with the standard deviation σ of the imaging system PSF $|h(\boldsymbol{\rho})|^2$. The asymptotic $1/\sqrt{N}$ decrease in width indicates a resolution enhancement at the SQL.

5. NEAR- AND FAR-FIELD CORRELATION MEASUREMENTS

With the full measurement of the correlation function in Eq. (3) of the article, spatial correlations of the OCM state can be analyzed. A double-slit of 200 μm line width is used as object. The OCM state shows in Fig. S1(a) position correlations along the x-direction orthogonal to the slits. This can be understood in terms of a 1-D version of Eq. (3) with $N = 2$, where the image is encoded in the centroid $\boldsymbol{X}$ (diagonal) and independence in $\boldsymbol{\xi}_1$ (anti-diagonal) is present. Both inner slit edges and the central dark separation are visible, vignetted by the pump beam shape. Replacing the imaging lens L_3 in the setup by a far-field lens of 400 mm focal length placed in this distance in front of the detector, far-field correlations of Fig. S1(b) are measured. Strong position correlations are observed in agreement with Eq. (6) of the article. Furthermore, comparing the diagonal of this biphoton diffraction pattern to a measurement with coherent light at 405 nm in Fig. S1(c) yields almost identical results, confirming the theoretically predicted relevance of the twice smaller de Broglie wavelength. A related result was obtained in [4].

REFERENCES

1. J. Goodman, *Introduction to Fourier Optics*, McGraw-Hill physical and quantum electronics series (W. H. Freeman, 2005).
2. M. Tsang, "Quantum Imaging beyond the Diffraction Limit by Optical Centroid Measurements," Phys. Rev. Lett. **102**, 253601 (2009).
3. C. H. Monken, P. H. Souto Ribeiro, and S. Pádua, "Transfer of angular spectrum and image formation in spontaneous parametric down-conversion," Phys. Rev. A **57**, 3123–3126 (1998).
4. M. D'Angelo, M. V. Chekhova, and Y. Shih, "Two-photon diffraction and quantum lithography," Phys. Rev. Lett. **87**, 013602 (2001).